

# ELECTRON MULTIPACTING CAN EXPLAIN THE PRESSURE RISE IN THE ANKA COLD BORE SUPERCONDUCTING UNDULATOR

S. Casalbuoni\*, S. Schleede, D. Saez de Jauregui, M. Hagelstein  
Forschungszentrum Karlsruhe, Karlsruhe, Germany

## Abstract

Preliminary studies performed with the cold bore superconducting undulator installed in the ANKA storage ring suggest that the beam heat load is mainly due to the electron wall bombardment. Electron bombardment can both heat the cold vacuum chamber and induce an increase in the pressure because of gas desorption. In this contribution we compare the measurements of the pressure in a cold bore performed in the electron storage ring ANKA with the prediction obtained using the equations of gas dynamic balance in a cold vacuum chamber exposed to synchrotron radiation and electron bombardment. The balance results from two competitive effects: the photon and electron desorption of the gas contained in the oxide layer of the chamber wall and of the gas cryosorbed, and the cryopumping of the cold surface. We show that photodesorption alone cannot explain the pressure rise observed and that electron multipacting is needed.

## INTRODUCTION

A cold bore superconducting undulator is installed in the ANKA storage ring since 2005 [1]. The beam heat load and the pressure in the cold vacuum chamber have been monitored since then. A correlation between the heat load and the pressure is observed. A simple model of electron bombardment appears to be consistent with the beam heat load and pressure rise observed during normal user operation [2].

In this paper we solve the equations of gas dynamic balance in a cold vacuum chamber exposed to synchrotron radiation and electron bombardment. We show that the pressure rise observed can be explained by the occurrence of electron multipacting and not by photodesorption.

## MODEL

The equations of gas dynamic balance inside a vacuum chamber can be written as (see Ref. [4, 5] and references therein):

$$\begin{aligned} V \frac{dn}{dt} &= q + q'(s) - \alpha S(n - n_e(s, T)) + u \frac{d^2 n}{dz^2}; \\ A \frac{ds}{dt} &= \alpha S(n - n_e(s, T)) - q'(s) \end{aligned} \quad (1)$$

\*sara.casalbuoni@iss.fzk.de

where  $n$  is the volume gas density,  $s$  the surface density of the cryosorbed gas,  $V$  the vacuum chamber volume,  $A$  the vacuum chamber wall area,  $q$  is the primary beam induced desorption flux,  $q'$  the secondary beam induced desorption flux (desorption of cryosorbed molecules),  $\alpha$  the sticking coefficient,  $S = A\bar{v}/4$  is the ideal wall pumping speed,  $\bar{v}$  is the mean molecular speed,  $n_e$  the thermal equilibrium gas density, and  $u$  the specific vacuum chamber conductance per unit axial length. We consider in the following the gas to consist only of  $H_2$ . The beam induced desorption flux consists of photon (PSD) and electron (ESD) stimulated desorption:

$$\begin{aligned} q &= \eta \dot{\Gamma} + \phi \dot{\Theta}; \\ q' &= \eta' \dot{\Gamma} + \phi' \dot{\Theta}; \end{aligned} \quad (2)$$

where  $\eta$  and  $\eta'$  are the primary and secondary electron stimulated desorption yields,  $\dot{\Gamma}$  is the electron flux,  $\phi$  and  $\phi'$  are the primary and secondary photodesorption yields, and  $\dot{\Theta}$  is the photon flux.

The specific vacuum chamber conductance per unit axial length is given by  $u = A_c D$ , where  $D = 2/3 A_c \bar{v}$  is the Knudsen diffusion coefficient being  $A_c$  the area of the rectangular cross section of the vacuum chamber. Axial diffusion can be neglected when  $DA_c/L^2 < S\alpha$  [4], which means:

$$\frac{8}{3} \frac{A_c^2}{AL^2} < \alpha. \quad (3)$$

Experimental values of the sticking coefficient for  $H_2$  at 4.2 K indicate  $\alpha > 0.02$  [6]. Even considering  $\alpha = 0.02$  condition (3) is satisfied for the geometry of the undulator vacuum chamber where  $L = 1.8$  m and for a gap of 29 mm,  $A_c = 0.00191$  m<sup>2</sup> and  $A = 0.266$  m<sup>2</sup>. Therefore in the following we neglect axial diffusion  $ud^2n/dz^2 \approx 0$ .

## RESULTS

Various simulations have been performed solving Eqs. 1 using the values listed in Table I as input parameters. Most of the input parameters as the photon and electron primary and secondary desorption yield, as well as the sticking coefficient are very difficult to be measured. In the literature they are found within a large range of values. The photon primary desorption yield  $\phi$  and the ratio of the secondary photodesorption yield  $\phi'$  with the sticking coefficient  $\alpha$  have been measured on a copper electroplated stainless steel liner by Anashin et al. [8] to vary in the

Light Sources and FELs

T15 - Undulators and Wigglers

range  $2 \cdot 10^{-4} \leq \phi \leq 5 \cdot 10^{-2}$ . In Ref. [9] are reported the measurements of the primary electron desorption yield  $5 \cdot 10^{-4} \leq \eta \leq 10^{-1}$  and the sum of the primary and secondary electron desorption yields over the sticking coefficient  $2 \cdot 10^{-2} \leq (\eta + \eta')/\alpha \leq 10$  for the Large Hadron Collider (LHC) beam screen (copper electroplated stainless steel liner) at 12 K as functions of the electron dose. In a more recent work [10] a measurement of the sticking coefficient as a function of H<sub>2</sub> coverage at about 2 K on the LHC beam screen show that  $0.25 \leq \alpha \leq 0.52$ .

The idea is to change the input parameters within the range of values found in the literature and to compare the pressure simulated with the one measured. If not differently specified, we have used the values indicated in the column 'fixed' and we have performed different simulations by varying the parameters shown in Table I within the values indicated in the columns 'min' and 'max'. The

Table 1: Values used as input parameters in Eqs.1.

	min	max	fixed
$n_0$ ( $10^{13}$ mol/m <sup>3</sup> )			1.2
$s_0$ ( $10^{19}$ mol/m <sup>2</sup> )	1.4	1.66	1.66
$\alpha$	.3	.5	.5
$\phi$	0.0001	.01	0.0002
$\phi'$	0.01	.1	0.09
$\eta$	0.001	.003	0.002
$\eta'$	0.001	.005	0.003
$\dot{\Gamma}_0$ ( $10^{15}$ ph/sec)			4.6
$\dot{\Theta}_0$ ( $10^{17}$ el/sec)			6.
$\tau$ (sec)			47857
$\tau_{el}$ (sec)	8000	16000	11000

volume gas density  $n$  at a temperature  $T$  is related to the pressure measured at room temperature by:

$$n = \frac{P}{k_B \sqrt{T T_{RT}}} . \quad (4)$$

The value of  $n_0$  is obtained by Eq. 4 with  $P = 6 \times 10^{-11}$  mbar. We have assumed  $n_e(s, T) = n_0$ . The surface coverage at equilibrium  $s_0$  is deduced by the measured adsorption isotherms of H<sub>2</sub> on copper plated stainless steel at 4.2 K from Ref. [11].

The photon flux is proportional to the beam current, so we consider it to decay exponentially with time as :  $\dot{\Gamma} = \dot{\Gamma}_0 \exp -t/\tau$  where  $\tau$  is the beam lifetime which we assume here about 13 hours. We assume that the electron flux also decays exponentially in time:  $\dot{\Theta} = \dot{\Theta}_0 \exp -t/\tau_{el}$ . We have varied  $\tau_{el}$  between 2 and 4 hours. For the ANKA cold bore vacuum chamber with gap = 29 mm and average beam current  $I = 100$  mA, the photon flux impinging on the lower and upper surfaces is  $\dot{\Theta}_0 = 4.6 \cdot 10^{15}$  photons/s.

If the heat load observed is generated by electron bombardment and assuming a mean electron energy  $\Delta W = 10$  eV (for a typical  $3.6 \times 10^9$  electrons/bunch), the estimated electron flux for a heat load of  $P = 1$  W is  $\dot{\Gamma} \approx$

$6 \times 10^{17}$  electrons/s. We assume then  $\dot{\Gamma}_0 = 6 \times 10^{17}$  electrons/s.

The pressure rise obtained considering only photodesorption is plotted in Fig. 1. Simulations considering only photodesorption ( $\dot{\Theta}_0 = 0$  el/sec), and using the 'fixed' values of the input parameters as in Table I varying the sticking coefficient  $\alpha$  (see Fig. 1 a)), the primary photodesorption yield  $\phi$  (see Fig. 1 b)), the secondary photodesorption yield  $\phi'$  (see Fig. 1 c)), and the initial value of the H<sub>2</sub> surface coverage  $s_0$  (see Fig. 1 d)) have been performed. The results are compared with the measurements (green circles) which span in a large range of values. The typical observed behaviour is indicated by the three curves with green circles. Taking into account of photodesorption only

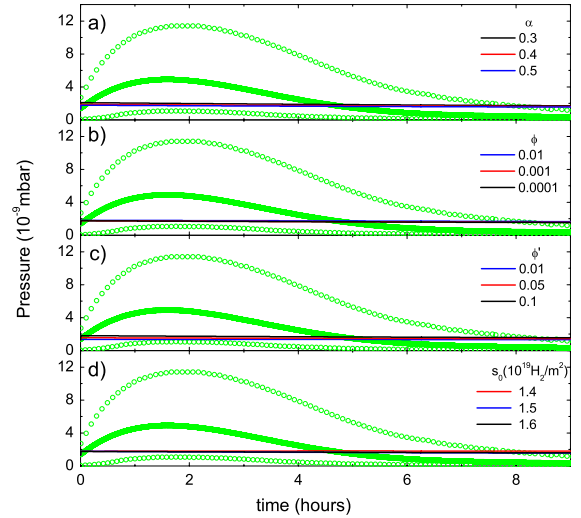


Figure 1: Pressure in the cold vacuum chamber as a function of time. The green circles indicate the typical behaviour and range of measured values. The simulations shown in these plots consider only photodesorption ( $\dot{\Theta}_0 = 0$  el/sec) and are obtained using the 'fixed' values of the input parameters as in Table I varying a) the sticking coefficient  $\alpha$ , b) the primary photodesorption yield  $\phi$ , c) the secondary photodesorption yield  $\phi'$ , d) and the initial value of the H<sub>2</sub> surface coverage  $s_0$ .

( $\dot{\Theta}_0 = 0$  el/sec), by varying the input parameters in the range indicated in Table I it is impossible to reproduce the observed behaviour of the pressure.

The results obtained considering also electron desorption are shown in Fig. 2. By varying the input parameters in the range indicated in Table I it is in this case possible to reproduce the observed behaviour of the pressure. The measurements are well reproduced by using a decay time of the electron desorbing H<sub>2</sub> from the surface  $\tau_{el}$  of 8000 sec. This implies as a result the multipacting shown in Fig. 3, where the flux of the electrons desorbing H<sub>2</sub> molecules from the cold surface is shown as a function of the beam current. Multipacting occurs in Fig. 3 at beam currents

higher than about 120 mA.

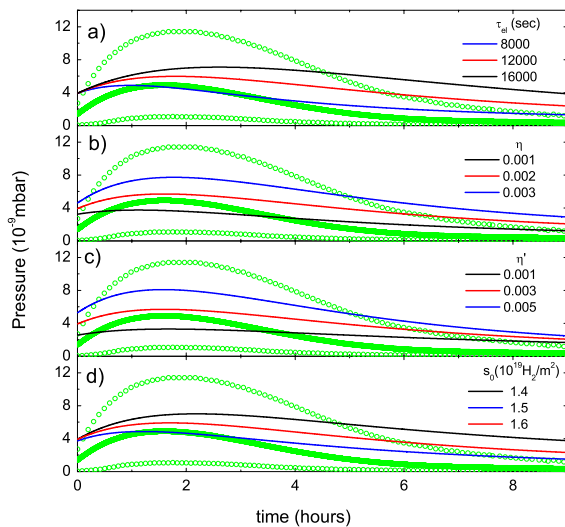


Figure 2: Pressure in the cold vacuum chamber as a function of time. The green circles indicate the typical behavior and range of measured values. The simulations shown in these plots are obtained considering also electron desorption and using the 'fixed' values of the input parameters as in Table I varying a) the decay time of the electron desorbing  $H_2$  from the surface  $\tau_{el}$ , b) the primary electron desorption yield  $\eta$ , c) the secondary electron desorption yield  $\eta'$ , d) and the initial value of the  $H_2$  surface coverage  $s_0$ .

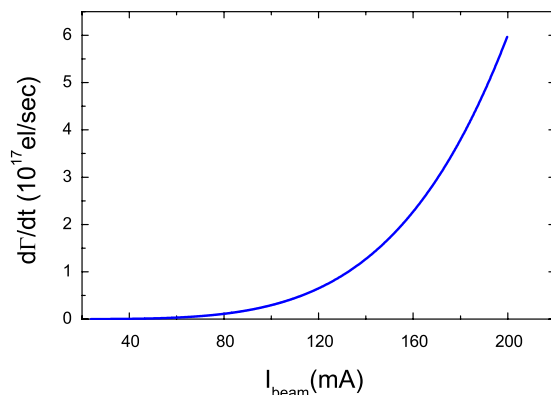


Figure 3: Flux of the electrons desorbing  $H_2$  molecules from the surface as a function of the beam current.

## CONCLUSIONS AND OUTLOOK

A simple model of electron bombardment appears to be consistent with the beam heat load and pressure rise observed in the cold bore of the superconducting undulator

installed at ANKA. The nature of the electron bombardment is not clear [13]. We have shown that to reproduce the pressure measurements it is necessary to include electron multipacting, which implies a decay time of the electron flux  $\tau_{el}$  shorter than the beam lifetime  $\tau$ . Considering the simplified assumptions, for example the gas made by  $H_2$  only and the poor quality of the measurements the agreement between simulations and measurements is satisfying. A refinement of the model makes sense once more accurate and controlled measurements will be available with the planned cold vacuum chamber (COLDDIAG) to be installed in a storage ring, implemented with the following diagnostics: i) retarding field analyzers to measure the electron energy and flux, ii) temperature sensors to measure the total heat load, iii) pressure gauges, iv) and a mass spectrometer to measure the gas content [12].

## ACKNOWLEDGEMENTS

The authors are grateful to Frank Zimmermann (CERN) for useful discussions in the initial phase of this project.

## REFERENCES

- [1] S. Casalbuoni et al., *Phys. Rev. ST Accel. Beams* **9**, 010702 (2006).
- [2] S. Casalbuoni et al., *Phys. Rev. ST Accel. Beams* **10**, 093202 (2007).
- [3] The pressure values reported in this paper are measured at room temperature. The corresponding values at low temperature can be obtained applying the Knudsen relation  $P(T) = (T[K]/300\text{ K})^{1/2} P(300\text{ K})$ .
- [4] W.C. Turner, Proceedings of PAC 1993, Washington, D.C., USA 1993.
- [5] I.R. Collins and O.B. Malyshev, LHC Project Report 274, 2001.
- [6] S. Andersson, L. Wilzén, M. Persson, J. Harris, *Phys. Rev. B* **40**, 8146 (1989); V.V. Anashin et al., *J. Vac. Sci. Techn.* **12** (4), 1663 (1994).
- [7] V.V. Anashin et al., *Vacuum* **48** (7-9), 785 (1996).
- [8] V.V. Anashin et al., *J. Vac. Sci. Techn.* **12** (5), 2917 (1994).
- [9] V. Baglin, B. Jenninger, LHC Project Report 721, 2004.
- [10] H. Tratnik, PhD thesis, Wien (2005).
- [11] E. Wallén, *J. Vac. Sci. Techn.* **14** (5), 2916 (1996).
- [12] S. Casalbuoni et al., Proceedings of EPAC 2008, Genoa, Italy 2008.
- [13] U. Iriso et al., this proceedings.